

Signature-Graph Networks

Ali Hamdi, Flora Salim, Du Yong Kim, and Xiaojun Chang

Abstract—We propose a novel approach for visual representation learning called Signature-Graph Neural Networks (SGN). SGN learns latent global structures that augment the feature representation of Convolutional Neural Networks (CNN). SGN constructs unique undirected graphs for each image based on the CNN feature maps. The feature maps are partitioned into a set of equal and non-overlapping patches. The graph nodes are located on high-contrast sharp convolution features with the local maxima or minima in these patches. The node embeddings are aggregated through novel Signature-Graphs based on horizontal and vertical edge connections. The representation vectors are then computed based on the spectral Laplacian eigenvalues of the graphs. SGN outperforms existing methods of recent graph convolutional networks, generative adversarial networks, and auto-encoders with image classification accuracy of 99.65% on ASIRRA, 99.91% on MNIST, 98.55% on Fashion-MNIST, 96.18% on CIFAR-10, 84.71% on CIFAR-100, 94.36% on STL-10, and 95.86% on SVHN datasets. We also introduce a novel implementation of the state-of-the-art multi-head attention (MHA) on top of the proposed SGN. Adding SGN to MHA improved the image classification accuracy from 86.92% to 94.36% on the STL10 dataset.

Index Terms—Visual Representation Learning, Graph Neural Networks.

I. INTRODUCTION

IN visual representation learning, Convolutional Neural Networks (CNN) have been widely utilised to extract effective feature representations from images. However, CNNs ignore useful global information due to the isotropic nature of their receptive fields [1] and, thus, CNNs are affected by challenging foreground and backgrounds noise. Recent CNN architectures have large sets of layers to adapt to the increasing size and complexity of training data [2]. Such complex and deep models usually suffer from overfitting when trained on relatively small data. Recently, the overfitting problem has been addressed by different techniques such as data augmentation [3]. However, traditional augmentation techniques are tackled by visual uncertainties in colours and shapes in images. For example, augmenting an image of a bird by changing colour may result in a bird of different group, or, rotating an image of a flower has no effect. To overcome these challenges, images can be represented as graphs to denote global features and integrated into CNN. Yet, traditional CNN cannot deal with such graphs of irregular structure. These CNN limitations can be solved using recent advances in graph neural networks or graph based methods.

Ali Hamdi, Flora Salim and Xiaojun Chang are with the School of Computing Technologies, RMIT University, Australia, ali.ali@rmit.edu.au, flora.salim@rmit.edu.au, xiaojun.chang@rmit.edu.au.

Du Yong Kim is with the School of Engineering, RMIT University, Australia, duyong.kim@rmit.edu.au.

Manuscript received October 14, 2021; revised 15 January 2022.

There are various graph representations such as region-based [4], part-based [5], and predefined skeleton [6]. Graph-based methods improved CNN performance as they capture important global features embedding to produce accurate image representations [4]. However, these graph architectures might misrepresent significant local structures and need high computational resources [2]. Besides, graph models were mainly developed to represent multiple objects in an image for tasks such as detection and tracking. There is less effort in representing the whole image as a feature vector based on graphs that the proposed SGN is addressing. These graph-designs have been accompanied by complex models, such as context-aware, attentional and memory-based, to enhance visual representation learning [7], [8], [9], [10], [11]. In contrast to these complex architectures, we propose to learn visual feature embeddings through straightforward and accurate signature-like graphs. We reinvent the idea of capturing global attentions to support the CNN extracted feature embeddings.

Signature-Graphs tend to have unique and similar representations for images from the same class and different from the others. We extract the CNN feature maps; then we partition them into a set of equal and non-overlapping patches. Each patch is represented by a node in the Signature-Graph. Fig. 1 visualises the construction of the Signature-Graphs. It shows a heat-map of an image feature map from which the nodes are located to connect the Signature-Graphs. These nodes represent sharp high-contrast features convolutional features with the local maxima in their respective patches. Similarly, the graph could be constructed with nodes of the local minima of different patches. To connect these nodes, two novel Signature-Graphs designs are proposed based on horizontal and vertical edge-connections. SGN offers a straightforward yet accurate method to learn useful visual features. It can be easily extended with other representation learning techniques. For example, multi-head attention (MHA) networks can be employed on top of the SGN to learn more useful features using attention mechanism. Other CNN baseline networks can also be combined with SGN. The experimental results show that SGN has significantly improved the accuracy of these methods.

In this paper, we present a set of contributions to the graph design, CNN vector augmentation, and global attentional feature computing, as follows:

- The proposed SGN augments CNN local features with graph-based global feature embeddings. Particularly, we introduce a new feature embedding method, Signature-Graphs, that capture unique global attentions via connections among different image regions.
- We implement a novel design architecture of SGN with the state-of-the-art MHA mechanism. Specifically, we

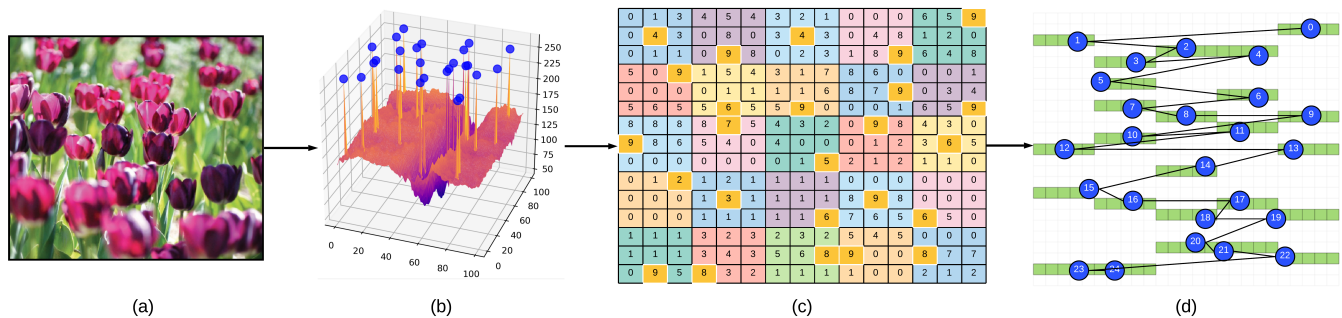


Fig. 1. (a) heat-map of an image feature map, (b) the heat-map with selected coordinates of convolution features with local maxima in different patches. (c and d) constructing Signature-Graphs of the selected nodes' coordinates to aggregate the feature embeddings.

feed the MHA with SGN output vectors as key vectors that capture more accurate attentions than using the existing method.

- We evaluate the proposed SGN on seven benchmark multi-class and binary image classification datasets. SGN achieves superior performance over existing methods.

II. RELATED WORK

Graph-based models have been widely used in multiple research tasks, such as multi-label recognition [7], skeleton-based action recognition [8], point-cloud semantic segmentation [9], large-scale object detection [12], 3D pose regression [10], and person re-identification [11]. Recently, graph-based models have been accompanied by context-aware, attentive and memory-based models. Chen *et al.*, [7] utilised graph convolutional network (GCN) for multi-label image recognition. Si *et al.*, [8] proposed an attention-based LSTM with GCN for skeleton-based action recognition. GCN with attention model has also developed in [9] for point cloud semantic segmentation. Xu *et al.*, [12] presented a spatial-aware graph relation network for object detection in large-scale data. These models capture important global features that support accurate image representations. The attention and memory weights are updated throughout the learning process. In contrast to the previous deep and complex architectures, we propose to learn visual embeddings via Signature-Graphs that are uncomplicated yet accurate compared to state-of-the-art visual representation methods. We present a simple implementation to learning important global features in comparison attention and memory-based complex approaches.

There are multiple image graph-based representations. These models try to represent the image in different ways, such as region-based [4], part-based [5], and predefined skeleton [6]. These approaches outperform CNN in encoding long relations between image regions [4], [8]. Motivated by these approaches we propose a new graph representation method, the so-called, Signature-Graphs. The designed Signature-Graphs tend to overcome the limitations of these previous graph architectures, such as losing significant local structures and the need for high computation resources. The Signature-Graphs tend to offer robust visual feature embeddings via undirected-graph design. Previous graph-based models were developed for

visual tasks with multiple objects in an image such as object detection and tracking. However, there is less effort in the case of dealing with the whole image with no predefined semantic labels. The proposed SGN solves this issue by augmenting the CNN vectors with the new Signature-Graphs feature vectors.

III. SIGNATURE-GRAPH NEURAL NETWORKS

The proposed SGN is designed as a mechanism to augment the CNN feature vectors with graph-based global information. Fig. 2 shows the proposed Signature-Graphs. Specifically, we propose to attach a Signature-Graph layer to each convolutional block. The Signature-Graph layer tends to extract global features that are missed in the CNN classical design of the receptive fields.

A. Convolutional Feature Extraction

SGN is a modified architecture of CNN. SGN starts with the extraction of the convolutional feature extraction. Typically, a CNN is composed of a series of convolutional and pooling layers to extract the significant features in an image I . The image I is characterised by I_h height, I_w width, and I_c colour channels. The CNN convolutional product is computed as a 2-dimensional matrix that contains the sum of the element-wise multiplication of the image I and a convolutional filter F that must have the F_c equals to the I_c .

$$Conv2D(I, F)_{x,y} = \sum_{i=1}^h \sum_{j=1}^w \sum_{k=1}^c K_{i,j,k} I_{x+i-1, j+j-1, k} \quad (1)$$

where, I and F are the image and convolutional filter, x and y denote the image coordinates, and h , w , and c are the image attributes. The $Conv2D$ in Eq. 1 learns a feature map of the image I . The output feature maps are then passed to a pooling layer to down-sample the image features. Pooling is using a sliding window, similar to the convolution, although it keeps the max or average of the pixels values instead of the multiplication.

CNNs are affected by the overfitting problem. This happens when a CNN based method extensively learns the convolutional features through a very complex architecture. In such a scenario, the learnt model performs poorly in the testing on

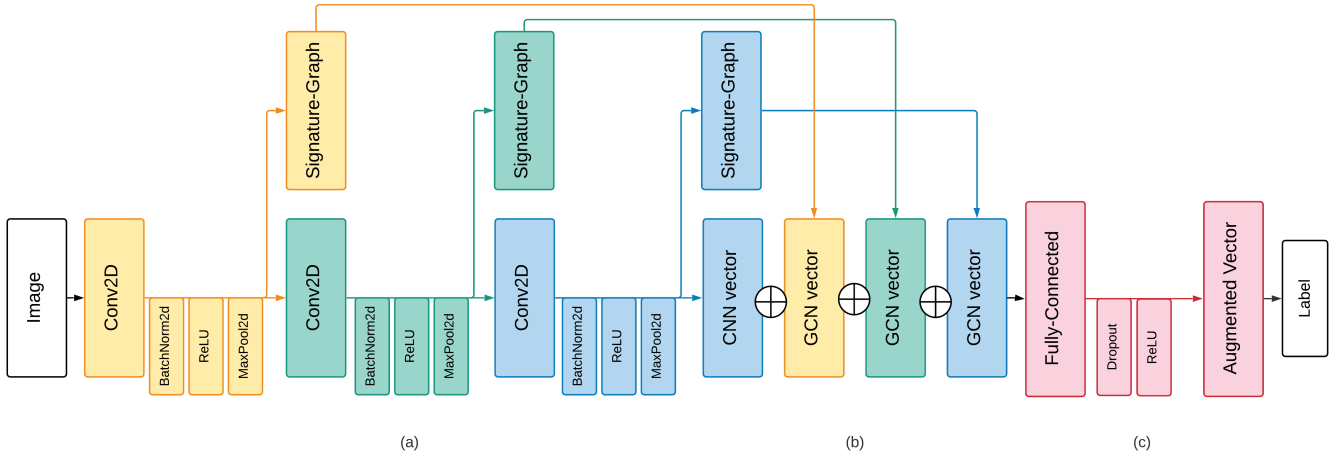


Fig. 2. SGN consists of three convolutional blocks (a). Each block is followed by batch normalisation, Relu activation, and max-pooling layers. The feature maps of each convolutional block are injected in the subsequent convolutional block and a Signature-Graph layer. The Signature-Graph layer computes the global features via a Signature-Graphs, as in Fig. 1. The output of the last convolutional block is concatenated with the output of the three Signature-Graph layers (b). A fully-connected layer is attached at the end of SGN to produce the final augmented feature vector.

unseen images. Therefore, we utilised a batch normalisation layer before the max-pooling layer to standardise the input pixel values. This normalisation process makes the feature maps to have a mean of zero and a standard deviation of one. This layer observes the learning statistics and updates the standardised data. We also add a non-linear Rectified Linear Unit (Relu) activation layer before the pooling process. The CNN final feature maps are flattened in a 1-dimensional vector and connected to a fully-connected layer. However, it is not practical to connect all the neurons with all possible region of the input features. This would make the process too complex with many weights to train. Therefore, CNNs depend on a receptive field [1]. The receptive field is simply a 2-dimensional kernel which contains the pixels that are fully-connected. Although this process enhances the convolutional feature learning, it limits the CNN to learn local features from different image regions. Therefore, in this paper, we propose to augment the CNN output feature vector with the global image feature through novel *Signature-Graph*.

B. Signature-Graphs

We propose to construct a unique graph from each feature map. In the following sub-sections, we explain three main components of the Signature-Graphs as follows:

- *Signature-Graph construction* sub-section discusses the selection of the nodes' coordinates and their correspondent visual features.
- *Spectral graph computing* sub-section introduces the computing of the Eigenvalues over the Laplacian matrix to normalise the node feature vector embeddings.
- *Multi-Head Attention* sub-section defines the employed multi-head attention mechanism and how the SGN contributes to it.

1) *Signature-Graphs Construction*: The output standardised and pooled convolutional feature maps are injected into a Signature-Graph layer. The Signature-Graph layer applies

graph spectral theory over the convolutional maps. In order to implement the spectral graph methods, we first construct a Signature-Graph. The feature map is divided into a set of equal and non-overlapping patches.

Each patch is a 2-dimensional array of convolutional features. Each patch is represented by one node in the graph. To select the node coordinates in the patch, we consider the feature with the local maxima and minima. The hypothesis behind these selections is that the local maxima and minima of the convolutional feature represents the highest-contrast points in the respective patches. Therefore, we suppose that positioning the graph nodes at these locations can offer effective representations due to the expected sharpness of these points. So, the Signature-Graph nodes can be,

$$V, X = \max(p_f) \rightarrow \max(p_f)_{row}; \forall p \in P \quad (2)$$

or,

$$V, X = \min(p_f) \rightarrow \min(p_f)_{row}; \forall p \in P \quad (3)$$

where P is a set of patches of the feature map, $\max(p_f)$ is the feature with the highest value in a patch, and $\min(p_f)$ refers to the feature that has the lowest value in a patch. The output V and X are the nodes and node attributes. The V nodes are computed as a set of CNN feature coordinates in the given patch, and their corresponding rows are employed as the node attributes X , as visualised in Fig. 1 (d). We utilised the computed V and their attributes X to construct the Signature-Graph, as in Eq. 4.

$$G = (V, E) \quad (4)$$

where G is the Signature-Graph, V the graph nodes, and E the graph edges that are computed based on the distances between the nodes' coordinates. G is an undirected graph.

We propose a new graph design to extract the most useful features from the above-explained G . We propose to connect the graph nodes through horizontal or vertical edges passing

across the image patches. The idea of connecting horizontal and vertical graph components is presented in multiple research studies, such as squaring a square [13] and planar graphs [14]. We assume that SGN with horizontal and vertical Signature-Graphs could capture unique latent connections between different local regions in an image. Later, in this paper, the experimental results show that SGN with horizontal and vertical edges outperform each other in different datasets.

2) *Spectral Graph Computing*: The constructed Signature-Graph has a set of spectral characteristics that can be computed through different matrices such as the degree matrix D , adjacency matrix A , and incidence matrix M . The degree matrix D is a diagonal matrix that contains the degree of each node in the graph. The adjacency matrix A , or connection matrix, has boolean representations of the node positions. The incidence matrix M represents the connections between the graph nodes and edges. The Laplacian matrix L is defined as:

$$\mathcal{L}_{n \times n} = D - A \quad (5)$$

where n denotes the number of nodes in the Signature-Graph. The Laplacian \mathcal{L} can be normalised as a Kirchhoff matrix, as follows:

$$\mathcal{L}_{ij}(G) = \begin{cases} 1 & \text{if } i = j \text{ and } d_j \neq 0 \\ -\frac{1}{\sqrt{d_i d_j}} & \text{if } i \text{ and } j \text{ are adjacent} \\ 0 & \text{otherwise} \end{cases} \quad (6)$$

where d is an element of the degree matrix D .

The Laplacian matrix satisfies $\mathcal{L} = M^T M$ with M is the incidence matrix, and M^T is its transpose. Elements in M are described as M_{ev} with e connects nodes i and j and v node as in Eq. 7.

$$M_{ev} = \begin{cases} 1, & \text{if } v = i \\ -1, & \text{if } v = j \\ 0, & \text{otherwise} \end{cases} \quad (7)$$

The eigendecomposition of \mathcal{L} with eigenvectors and eigenvalues λ can be computed as in Eq. 8

$$\begin{aligned} \lambda_i &= \mathbf{v}_i^T L \mathbf{v}_i \\ &= \mathbf{v}_i^T M^T M \mathbf{v}_i \\ &= (M \mathbf{v}_i)^T (M \mathbf{v}_i). \end{aligned} \quad (8)$$

We normalise the node embeddings with the eigenvalues of the graph based on a Fourier basis. Fourier basis eigenvectors and their corresponding eigenvalues Λ represent the direction and variance of the graph Laplacian. The decomposed eigenvectors are computed as a matrix $U \in R^{n \times n}$ that contains η_n where n dimension is the same as node counts. These eigenvectors have a natural signal-frequency interpretation for the graph. The spectral Fourier basis decomposition produces the matrix U that diagonalises the Laplacian as in Eq. 9, where Λ is a diagonal matrix of non-negative real eigenvalues, see Eq. 10, A is the adjacency matrix, and I is the input image.

$$\mathcal{L} = \text{diag}(A + I)^{-1} = U \Lambda U^T \quad (9)$$

$$A \vec{U} = \Lambda \vec{U} \quad (10)$$

An eigenvalue λ of each node in the Signature-Graph is multiplied in the corresponding row pixel values, computed as node attribute X , as in Eq. 11, producing the final node embeddings \hat{X} .

$$\hat{X} = \Lambda X \quad (11)$$

The spectral-normalised node embeddings are concatenated together in one Signature-Graph vector. This vector is concatenated with the CNN feature vector to achieve the augmentation objective. The final augmented vector is passed to a fully-connected layer.

Finally, the SGN concatenates the Signature-Graph vector \hat{X} and the CNN vector $Conv$.

$$f(I) = \hat{X} \frown Conv \quad (12)$$

where \frown denotes the concatenation process. We then apply the *Cross - Entropy* loss function that combines the Log Softmax and negative log likelihood loss.

$$Cross - Entropy = - \sum_{i=1}^n \sum_{j=1}^m y_{i,j} \log(\hat{y}_{i,j}) \quad (13)$$

where $y_{i,j}$ refers to ground-truth label of sample i belongs class j , and $\hat{y}_{i,j}$ is the SGN model prediction.

C. An Extension to Multi-Head Attention

SGN can be easily extended with other representation learning techniques, such as multi-head attention. The multi-head self-attention mechanism [15] learns the representation encoding into through a set of key-values pairs while both the keys \mathbf{K} and values \mathbf{V} are the encoder hidden states. It then map the encoded pairs of key and values vectors with query \mathbf{Q} vectors.

The output dot-product attention is computed as a weighted sum of the values. The weight of each value is calculated by the dot-product of the query with all the keys, as follows:

$$\text{Attention}(\mathbf{Q}, \mathbf{K}, \mathbf{V}) = \text{softmax} \left(\frac{\mathbf{Q} \mathbf{K}^T}{\sqrt{n}} \right) \mathbf{V} \quad (14)$$

We propose a novel mechanism to produce the multi-head attention key, value, and query vectors, as in Fig. 3. the proposed SGN is utilised to encode the key vectors from the convolutional maps. The convolutional feature vectors are used as the values. Positional encoding is applied on the convolutional feature to compute the query vectors.

$$\begin{aligned} \text{MHA}(Q, K, V) &= \text{Concat}(\text{head}_1, \dots, \text{head}_h) W^O \\ \text{head}_i &= \text{Attention} \left(Q W_i^Q, K W_i^K, V W_i^V \right) \end{aligned} \quad (15)$$

IV. EXPERIMENTAL RESULTS

We present extensive performance analyses on seven benchmark dataset, including ASIRRA, MNIST, Fashion-MNIST, CIFAR-10, CIFAR-100, STL-10, and SVHN. Fig. 2 shows the neural network end-to-end trainable architecture of SGN. We implement SGN with only three convolutional blocks, each of which has followed by batch normalisation, Relu activation,

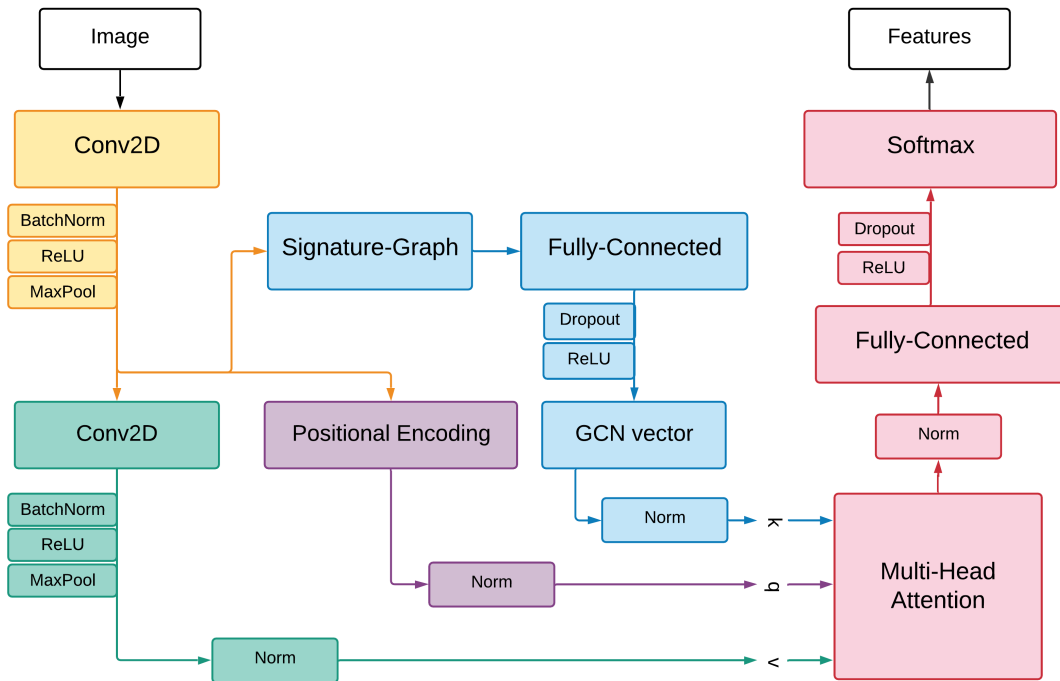


Fig. 3. Adding an SGN layer (blue coloured) to the implementation of the head model of Multi-Head Attention.

and max-pooling layers. The experimental results prove that this shallow architecture can outperform the state-of-the-art deep architecture on the ASIRRA data. The other datasets have lower resolution therefore we employ ResNet-50 as base model to SGN. SGN is also able to beat the recent attentional and variational auto-encoders. We have also extended the SGN with a multi-head attention as designed in Fig. 3.

A. Benchmark Experiment Results

1) *ASIRRA*: We experimented the proposed SGN on the ASIRRA (Animal Species Image Recognition for Restricting Access) dataset. Microsoft publishes this dataset for binary classification. ASIRRA is a balanced dataset having, for each class, 12,500 and 1,000 images for training and testing, respectively. Table I shows the experimental results using the binary image classification dataset ASIRRA. Table I shows the best result of using SGN with 1 layers, *horizontal* design, and local *maxima*. SGN outperforms state-of-the-art networks with 99.65%. flexgrid2vec [2] comes in the second rank with 98.8%. Comparison to flexgrid2vec is important because it implements GCN over image patches. These results support the significance of the utilisation of the graph-based feature learning for image classification against the other deep CNN architectures. Besides, the table lists the accuracy scores by multiple state-of-the-art deep networks such VGG [16], Inception [17], DenseNet [18], and NASNet [19]. The proposed SGN outperforms all of these deep networks.

2) *MNIST*: MNIST (Modified National Institute of Standards and Technology) dataset is composed of handwritten digits. It has 60,000 images for training and 10,000 for testing. The images are all in the size of 28×28 pixels.

TABLE I
CLASSIFICATION ACCURACY (TOP 1) RESULTS ON ASIRRA DATA.

Model	Test Accuracy
VGG16 [16]	82.2%
VGG19 [16]	88.2%
InceptionV3 [17]	97.2%
DenseNet121 [18]	94.3%
MobileNet [20]	98.4%
NASNetMobile [19]	97.9%
flexgrid2vec [2]	98.8%
SGN	99.65%

This dataset has been widely utilised to evaluate the visual pattern recognition models. Table II lists the benchmark results of the state-of-the-art methods using the MNIST dataset. We have experimented SGN with various layers, design, and node locations. In Table II, we report the best result of using SGN with 1 layers, *horizontal* edge connection, and local *maxima*. The proposed SGN outperforms the existing techniques and achieves state-of-the-art accuracy of 99.91%. The MNIST image classification error is reduced from 0.4 to 0.09. Although the current methods reach high performances on the MNIST dataset, SGN increases the accuracy yet higher. SGN outperforms other methods with different techniques such as stochastic optimisation of CNN [21], branching and merging CNN with homogeneous filter capsules [22], unsupervised learning of feature representation [23].

3) *Fashion-MNIST*: The Fashion-MNIST [33] dataset has been recently utilised to evaluate the image classification models. Fashion-MNIST has 50,000 images for training and

TABLE II
CLASSIFICATION ACCURACY (TOP 1) RESULTS ON MNIST.

Model	Test Accuracy
ProjectionNet [24]	95%
ANODE [25]	98.2%
Novikov et al., [26]	98.2%
Baikal [27]	99.47%
Neupde [28]	99.49%
TextCaps [29]	99.71%
SpinalNet [30]	99.72%
LocalLearning [31]	99.74%
CapsNet [32]	99.75%
SOPCNN [21]	99.83%
Branching/Merging CNN [22]	99.84%
C-SVDDNet [23]	99.6%
SGN	99.91%

10,000 for testing. Each image is a 28×28 grayscale. Fashion-MNIST covers 10 classes of different clothes such as T-shirt, trousers, pullover, and dress.

Table III shows the experimental results using the Fashion-MNIST dataset. Although the Fashion-MNIST dataset is more challenging than the MNIST the proposed SGN significantly outperforms the state-of-the-art methods. Table III lists the best result of using SGN with 1 layers, *vertical* design, and local *maxima*. SGN achieves the highest accuracy of 98.55%. SpinalNet [30] has 85.98% and 86.61% with different configurations. Neupde [28] also has different results of 88.33% and 92.40% with around 5% less accuracy than the proposed SGN. We present SGN as a vector-augmentation technique that complements the efforts of data augmentation methods. Random erasing data augmentation [34] utilised different, achieving 96.35% as its highest accuracy. The random erasing method employed other image classification deep architecture such as ResNet and ResNeXt by which random erasing achieves 95.99% and 96.21%, respectively. Using only three convolutional layers with the proposed Signature-Graph method achieves the best accuracy having a new state-of-the-art result.

TABLE III
CLASSIFICATION ACCURACY (TOP 1) RESULTS ON FASHION-MNIST.

Model	Test Accuracy
Spinal FC (10) [30]	86.61%
MLP 256-128-100 [28]	88.33%
Xiao et al., [35]	89.70%
Shake-Shake [36]	91.4%
ResNet18 [37]	92.00%
Neupde [28]	92.40%
TextCaps [29]	93.71%
DeepCaps [38]	94.46%
SpinalNet [30]	94.68%
LocalLearning [31]	95.47%
E2E-3M [39]	95.92%
ResNet + RE [34]	95.99%
WRN + RE [34]	96.35%
Random Erasing (RE) [34]	96.35%
SGN	98.55%

4) *CIFAR-10 and CIFAR-100*: We also test the proposed SGN on the CIFAR-10 [40] dataset. CIFAR-10 consists of 60,000 images. The images are in size 32×32 and divided into 50,000 for training and 10,000 for testing. CIFAR-10 has 10 categories such as air-plane, automobile, bird, cat, deer, dog, frog. The categories are mutually exclusive with no overlapping. The CIFAR-100 is similar to the CIFAR-10, while having 100 classes containing 600 images each.

Table IV lists the benchmark results using the CIFAR-10 dataset and the state-of-the-art methods. Although we have experimented SGN with various parameter values, Table IV reports the best result of using SGN with 1 layers, *horizontal* design, and local *maxima* for node localisation. The proposed SGN outperforms the existing methods achieving 95.26%. SGN can be described as a CNN with a patch-based Signature-Graph. DeepInfoMax [41] is one of the recent patch-based visual representation learning. As can be seen in Table IV, DeepInfoMax has 52.84%, 70.60%, 73.62%, and 75.57% accuracy based on different configurations and loss functions. Moreover, SGN outperforms other state-of-the-art feature learning methods such as AutoEncoder (AE), Adversarial AE, Variational AE, and β -VAE those have achieved 55.78%, 57.19%, 57.89%, and 60.54%, respectively. SGN also has better accuracy than recent studies such as Baikal [27] with 84.53%, Generic Feature Extractors (GFE) [42] with 89.1%, and CapsNet [32] with 89.4%. Generative adversarial neural networks (GANs) have recently achieved high performances in image representation learning. However, the proposed SGN outperforms recent GANs such as BiGAN [43], [44] with 62.74% and DCGAN [45] with 82.8%. APAC [46] is another work based on data augmentation. It proposes a methodology of learning augmented data. SGN has better accuracy with the proposed vector-augmentation technique. SGN has also outperformed recent work such as MIM [47], CLS-GAN [48], DSN [49], and BinaryConnect [50]. On the CIFAR-100, SGN has achieved 84.71% outperforming recent studies such as MixMatch [51] Mish [52], DIANet [53], and ResNet-1001 [54]. Table V shows more experimental results on the CIFAR-100. We have experimented SGN with various settings. In Table V, SGN has the best results with 1 layers, *horizontal* design, and local *maxima*.

5) *STL-10*: The STL-10 [64] is prepared for image recognition model evaluation. STL-10 has fewer labelled training examples. It has 5,000 images for training and 8,000 for testing, over 10 classes. The STL-10 has 100,000 unlabelled images for unsupervised learning. However, in this paper, we did not use any of these unlabelled images. The STL-10 5,000 and 8,000 images are in the size of 96×96 and are acquired for the ImageNet. Table VI lists the evaluation results using the STL-10 dataset using SGN with 1 layers, *horizontal* edge connections, and node located on local *maxima*. SGN outperforms the state-of-the-art methods. Consistently with the benchmark results on CIFAR-10, SGN has managed to outperform different methodologies such as the patch-based DeepInfoMax [41], Autoencoders [43], [65], [55], [56], [44], and GAN [43], [44]. The DeepInfoMax has scored 28.09%, 61.92%, 65.93%, and 67.08%. SGN outperforms all of these results with 70.94% accuracy.

TABLE IV
CLASSIFICATION ACCURACY (TOP 1) RESULTS ON CIFAR-10.

Model	Test Accuracy
AutoEncoder (AE)	55.78%
Adversarial AE [43]	57.19%
β -VAE [55], [56]	57.89%
ANODE [25]	60.6%
BiGAN [43], [44]	62.74%
DeepInfoMax (infoNCE) [41]	75.57%
DenseNet [18]	77.79%
DCGAN [45]	82.8%
Scat + FC [57]	84.7%
FPID [58]	89.06%
GFE [42]	89.1%
CapsNet [32]	89.4%
MP [59]	89.07%
VGG-13 (Spinal FC)	89.16%
ResNet-34 [37]	89.56%
APAC [46]	89.70%
MIM [47]	91.5%
CLS-GAN [48]	91.7%
DSN [49]	91.8%
BinaryConnect [50]	91.7%
Mish [52]	92.20%
SGN	95.26%

TABLE V
CLASSIFICATION ACCURACY (TOP 1) RESULTS ON CIFAR-100.

Model	Test Accuracy
DSN [49]	65.4%
Unsharp Masking [60]	60.36%
ResNet-50 [54]	67.06%
GFE [42]	67.7%
MIM [47]	70.8%
MixMatch [51]	74.10%
Mish [52]	74.41%
Stochastic Depth [61]	75.42%
Exponential Linear Units [62]	75.7%
DIANet [53]	76.98%
Evolution [63]	77%
ResNet-1001 [54]	77.3%
SGN	84.71%

6) *SVHN*: We have utilised the street view house numbers (SVHN) dataset to evaluate the proposed SGN. The SVHN contains 630,420 house numbers images. Table VII lists the benchmark results on the cropped format of the SVHN with 32×32 pixels. The SVHN official split contains 73,257 and 26,032 image for training and testing, respectively. SGN has the best accuracy of 95.86% when using 1 layers, *vertical* design, and local *minima*. SGN outperforms existing methods such as RetNet, DANN, and DWT.

B. Ablation Study

SGN has been implemented with two versions of network architecture with different number of convolutional blocks and edge-connection design. We have changed the network architecture design based on four criteria, as follows:

TABLE VI
CLASSIFICATION ACCURACY (TOP 1) RESULTS ON STL-10 DATASET.

Model	Test Accuracy
Adversarial AE [43]	43.89%
Variational AE [65]	46.47%
AE	46.82%
β -VAE [55], [56]	46.87%
BiGAN [43], [44]	58.48%
DeepInfoMax (DV) [41]	61.92%
DeepInfoMax (JSD) [41]	65.93%
DeepInfoMax (infoNCE) [41]	67.08%
ResNet18 [66]	72.66%
Second-order Hyperbolic CNN [67]	74.3%
SOPCNN (RA) [68]	88.08%
FixMatch [68]	89.59%
SESN [69]	91.49%
NSGANetV2 [70]	92%
FixMatch (RA) [68]	92.02%
SGN	94.36%

TABLE VII
CLASSIFICATION ACCURACY (TOP 1) RESULTS ON SVHN DATA.

Model	Test Accuracy
Asymmetric Tri-Training [71]	90.83%
ReNet+LSTM [72]	94.10%
DenseNet [18]	94.19%
WRN-OE [73]	94.19%
WRN [74]	94.50%
ReNet+GRU [72]	95.16%
Farhadi et al., [75]	94.62%
FPID [58]	95.67%
E-ABS [76]	89.20%
DANN [77]	91.00%
Associative Domain Adaptation [78]	91.80%
SE-a [79]	91.92%
SE-b [79]	95.62%
CLS-GAN [48]	94.02%
DWT-MEC [80]	94.62%
SGN	95.86%

- Node coordinates of local maxima and minima of the CNN features in the image patches.
- Visual feature embeddings via horizontal and vertical Signature-Graphs.
- The number of the SGN layers is experimented on of one-, two-, or three-layer.
- Using Signature-Graph layers with and without skip connection.
- Using SGN with pre-trained based models as well as the multi-head attentional mechanism.
- Patch size is experimented on 6×6 and 10×10 .

1) *Node Embedding and Edge Connection*:: Table VIII compares the SGN performance according to different node-embedding based on local maxima and minima of the CNN features. Using horizontal mode over local maxima-based nodes has the best results with 98.55% and 95.26% in the Fashion-MNIST and CIFAR-10 datasets, respectively. Signature-Graph designed on local maxima, and horizontal edge-connection outperformed other ablations. Fig. 4 has three rows where the first row shows four sample images from

TABLE VIII
USING SGN WITH LOCAL MAXIMA AGAINST MINIMA ON THE FASHION-MNIST AND CIFAR-10.

Layers	Edge-connection Mode	Fashion-MNIST (Maxima)	Fashion-MNIST (Minima)	CIFAR-10 (Maxima)
1	Horizontal	98.55%	93.24%	95.26%
2	Horizontal	93.04%	92.91%	84.27%
3	Horizontal	92.38%	92.78%	86.26%
1	Vertical	97.08%	92.86%	89.13%
2	Vertical	94.82%	91.90%	88.05%
3	Vertical	95.11%	93.01%	87.70%

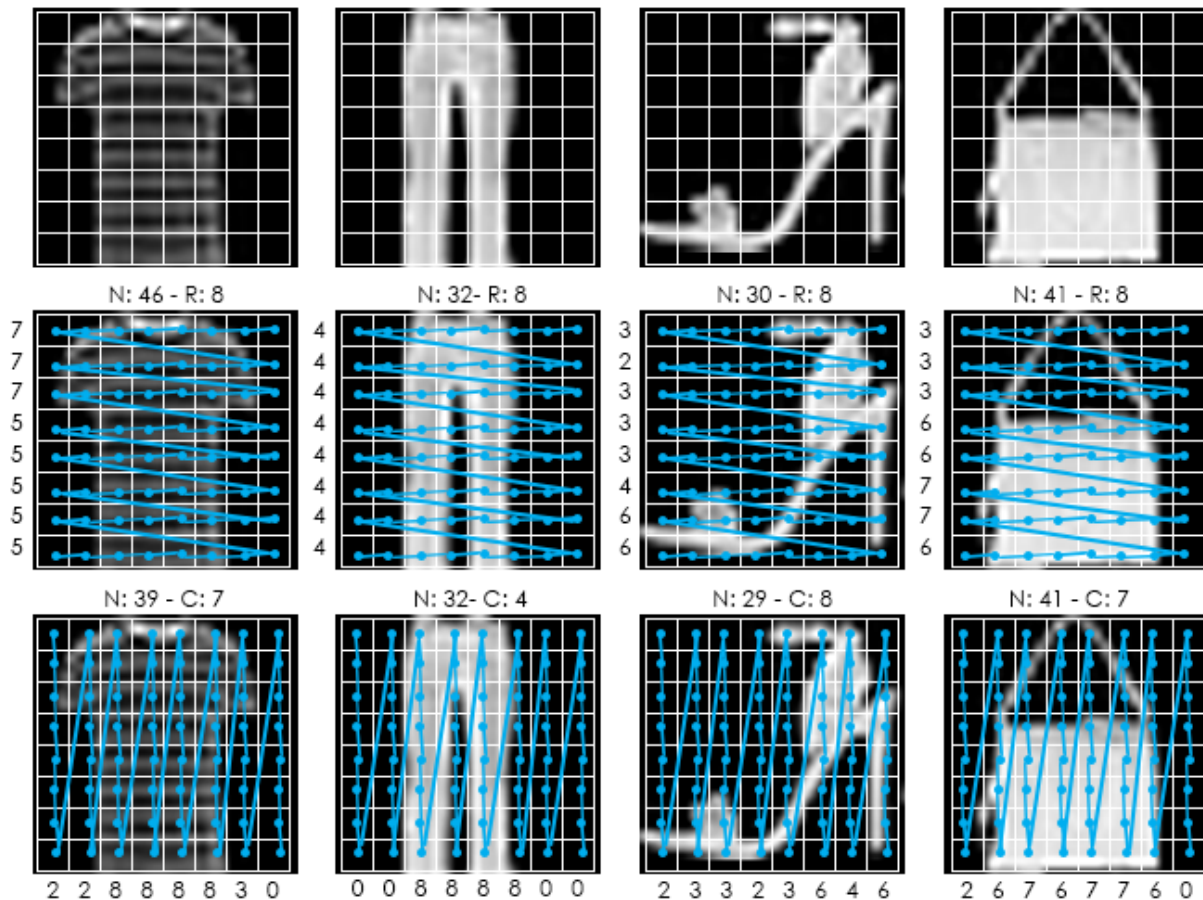


Fig. 4. Using Signature-Graph with horizontal and vertical edge-connection modes on four samples from the Fashion-MNIST dataset. The first row shows original images sliced into equal, non-overlapping patches. The second and third rows visualise the horizontal and vertical edge connection designs of Signature-Graph. We added the statistics on how many non-empty rows (R) and columns (C) above each image. We have also calculated the number of non-empty patches in each row (horizontal) and column (vertical) designs.

the Fashion-MNIST dataset, the second row visualises the horizontal Signature-Graph, and the third one visualises the vertical design. The pixel distribution over rows tends to be better than columns. Usually, every row has non-empty regions. In contrast, many columns have no foreground values. These facts support the superiority of horizontal SGN over vertical design. Fig. 4 shows counts of non-empty image patches in each row (horizontal) and column (vertical) designs. The totals of non-empty nodes and full rows or columns are given on top of each image. For example, the t-shirt image has higher values of nodes and rows using the horizontal Signature-Graph than the vertical one. These numbers of nodes

(patches) and horizontal rows or vertical columns directly impact the feature space.

2) *SGN Layers and Skip Connection*: We also tested the proposed SGN with one, two and three Signature-Graph layers. Table VIII shows that using one layer of the proposed horizontal Signature-Graph has the best results over one or three layers on the Fashion-MNIST dataset with 98.55% outperforming the vertical design. Using two Signature-Graph layers produces lower accuracy than the three-layer architecture. The latter one has 95.11% and 93.01% outperforming the two-layer method on the vertical SGN with maxima- and minima-based node locations, respectively. We tested SGN with skip

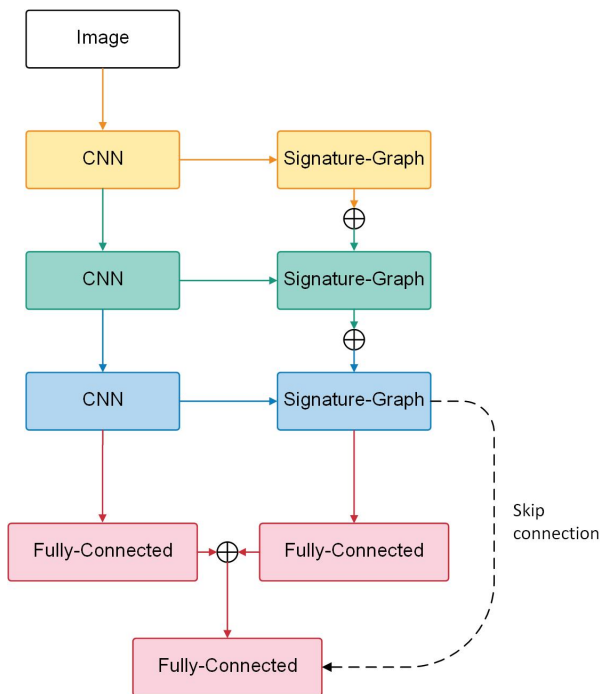


Fig. 5. Signature-Graph with skip connection.

connection as visualised in Fig. 5. Skip connection has become a standard component of CNN based visual representation methods. The skip connection is usually applied as addition and concatenation such as in ResNet [54] and DenseNet [18]. In this experiment, we feed the Signature-Graph features directly to the last fully-connected layer skipping other layers in between. This implementation adds the original Signature-Graph features to the final SGN feature vector allowing an alternative path for the gradient with back-propagation. Skip connection is helpful for CNN architecture convergence. The SGN with skip connection has 97.49% accuracy on the Fashion-MNIST compared to 98.55% without skip connection. This result outperforms all the ablations based on the vertical edge connection and minima-based node locations. However, using the Signature-Graph based on horizontal design and maxima node locations has the best accuracy without skip connection.

3) *SGN with Multi-head Attention*: We have also tested the proposed SGN with and without base and head model extensions. Using the MHA with the pre-trained EfficientNet has 86.92% while using SGN with same pre-trained model has 88.56%. Using MHA with ResNet50 has achieved 92.37% while adding SGN achieve the best accuracy of 94.36% on the STL-10 dataset.

4) *SGN with on Different Patch Sizes*: We have also investigated the impact of changing the patch size when partitioning the CNN feature maps to extract the Signature-Graph. This size controls how many nodes in the graph. For example, if the input image has 96×96 pixels, it has 16 and 10 nodes for the sizes of 6 and 10, respectively. This variation has an impact on the performance of the SGN. For example, the SGN has 97.08% and 92.65% for 6×6 and 10×10 patch sizes, when

TABLE IX
CLASSIFICATION ACCURACY (TOP 1) RESULTS USING THE SGN ON STL-10 TRAINED WITH BASE AND HEAD MODEL EXTENSIONS.

Basemodel	Test Accuracy
EfficientNet+MHA	86.92%
EfficientNet+SGN	88.56%
ResNet-50+MHA	92.37%
ResNet-50+MHA+SGN	94.36%

test on the Fashion-MNIST with the vertical design and local maxima nodes. Therefore, we utilised the 6×6 partitioning for all experiments to gain more useful Signature-Graph features.

V. CONCLUSION

Signature-Graph Network (SGN) contributes to graph feature embedding, CNN vector augmentation, and attention computing. SGN is a novel solution to the CNN limitation of the missing global structure information. SGN added a Signature-Graph layer on top of the convolutional block layers. The Signature-Graph extracts accurate feature embeddings through a signature-like graph from the convolutional feature map. The Signature-Graph utilises spectral graph theory to normalise the nodes' embeddings. We have compared the performance accuracy of the proposed SGN against a set of recent related works such as patch-based, auto-encoders, GAN, GCN, multi-head attention and data augmentation. The experimental results show that the proposed SGN end-to-end network using the Signature-Graph produces state-of-the-art image classification results. SGN works with a straightforward, shallow architecture of few convolution layers augmented and normalised with spectral Signature-Graph layers in comparison to these complex methods.

ACKNOWLEDGMENTS

Ali Hamdi is supported by RMIT Research Stipend Scholarship. This research is partially supported by Australian Research Council (ARC) Discovery Project *DP190101485*.

REFERENCES

- [1] W. Luo, Y. Li, R. Urtasun, R. Zemel, Understanding the effective receptive field in deep convolutional neural networks, in: *Advances in neural information processing systems*, 2016, pp. 4898–4906.
- [2] A. Hamdi, D. Y. Kim, F. Salim, flexgrid2vec: Learning efficient visual representations vectors, arXiv e-prints (2020) arXiv-2007.
- [3] I. Masi, A. T. Tran, T. Hassner, J. T. Leksut, G. Medioni, Do we really need to collect millions of faces for effective face recognition?, in: *European Conference on Computer Vision*, Springer, 2016, pp. 579–596.
- [4] Y. Li, A. Gupta, Beyond grids: Learning graph representations for visual recognition, in: *Advances in Neural Information Processing Systems*, 2018, pp. 9225–9235.
- [5] J. Gao, T. Zhang, C. Xu, Graph convolutional tracking, in: *Proceedings of the IEEE Conference on Computer Vision and Pattern Recognition*, 2019, pp. 4649–4659.
- [6] S. Yan, Y. Xiong, D. Lin, Spatial temporal graph convolutional networks for skeleton-based action recognition, in: *Thirty-Second AAAI Conference on Artificial Intelligence*, 2018.
- [7] Z.-M. Chen, X.-S. Wei, P. Wang, Y. Guo, Multi-label image recognition with graph convolutional networks, in: *The IEEE Conference on Computer Vision and Pattern Recognition (CVPR)*, 2019.

- [8] C. Si, W. Chen, W. Wang, L. Wang, T. Tan, An attention enhanced graph convolutional lstm network for skeleton-based action recognition, in: The IEEE Conference on Computer Vision and Pattern Recognition (CVPR), 2019.
- [9] L. Wang, Y. Huang, Y. Hou, S. Zhang, J. Shan, Graph attention convolution for point cloud semantic segmentation, in: The IEEE Conference on Computer Vision and Pattern Recognition (CVPR), 2019.
- [10] L. Zhao, X. Peng, Y. Tian, M. Kapadia, D. N. Metaxas, Semantic graph convolutional networks for 3d human pose regression, in: The IEEE Conference on Computer Vision and Pattern Recognition (CVPR), 2019.
- [11] Y. Shen, H. Li, S. Yi, D. Chen, X. Wang, Person re-identification with deep similarity-guided graph neural network, in: Proceedings of the European Conference on Computer Vision (ECCV), 2018, pp. 486–504.
- [12] H. Xu, C. Jiang, X. Liang, Z. Li, Spatial-aware graph relation network for large-scale object detection, in: The IEEE Conference on Computer Vision and Pattern Recognition (CVPR), 2019.
- [13] I. Stewart, Squaring the square, *Scientific American* 277 (1) (1997) 94–96.
- [14] S. Chaplick, T. Ueckerdt, Planar graphs as vpg-graphs, in: International Symposium on Graph Drawing, Springer, 2012, pp. 174–186.
- [15] A. Vaswani, N. Shazeer, N. Parmar, J. Uszkoreit, L. Jones, A. N. Gomez, L. Kaiser, I. Polosukhin, Attention is all you need, in: NIPS, 2017.
- [16] K. Simonyan, A. Zisserman, Very deep convolutional networks for large-scale image recognition, arXiv preprint arXiv:1409.1556 (2014).
- [17] C. Szegedy, V. Vanhoucke, S. Ioffe, J. Shlens, Z. Wojna, Rethinking the inception architecture for computer vision, in: Proceedings of the IEEE conference on computer vision and pattern recognition, 2016, pp. 2818–2826.
- [18] G. Huang, Z. Liu, L. Van Der Maaten, K. Q. Weinberger, Densely connected convolutional networks, in: Proceedings of the IEEE conference on computer vision and pattern recognition, 2017, pp. 4700–4708.
- [19] B. Zoph, V. Vasudevan, J. Shlens, Q. V. Le, Learning transferable architectures for scalable image recognition, in: Proceedings of the IEEE conference on computer vision and pattern recognition, 2018, pp. 8697–8710.
- [20] A. G. Howard, M. Zhu, B. Chen, D. Kalenichenko, W. Wang, T. Weyand, M. Andreetto, H. Adam, Mobilenets: Efficient convolutional neural networks for mobile vision applications, arXiv preprint arXiv:1704.04861 (2017).
- [21] Y. Assiri, Stochastic optimization of plain convolutional neural networks with simple methods, arXiv preprint arXiv:2001.08856 (2020).
- [22] A. Byerly, T. Kalganova, I. Dear, A branching and merging convolutional network with homogeneous filter capsules, arXiv preprint arXiv:2001.09136 (2020).
- [23] D. Wang, X. Tan, Unsupervised feature learning with c-svddnet, *Pattern Recogn.* 60 (C) (2016) 473–485. doi:10.1016/j.patcog.2016.06.001.
- [24] S. Ravi, Projectionnet: Learning efficient on-device deep networks using neural projections, arXiv preprint arXiv:1708.00630 (2017).
- [25] E. Dupont, A. Doucet, Y. W. Teh, Augmented neural odes, in: H. Wallach, H. Larochelle, A. Beygelzimer, F. d'Alché-Buc, E. Fox, R. Garnett (Eds.), *Advances in Neural Information Processing Systems* 32, Curran Associates, Inc., 2019, pp. 3140–3150.
- [26] A. Novikov, D. Podoprikin, A. Osokin, D. P. Vetrov, Tensorizing neural networks, in: C. Cortes, N. D. Lawrence, D. D. Lee, M. Sugiyama, R. Garnett (Eds.), *Advances in Neural Information Processing Systems* 28, Curran Associates, Inc., 2015, pp. 442–450.
- [27] S. Gonzalez, R. Miikkilainen, Improved training speed, accuracy, and data utilization through loss function optimization, in: 2020 IEEE Congress on Evolutionary Computation (CEC), IEEE, 2020, pp. 1–8.
- [28] Y. Sun, L. Zhang, H. Schaeffer, Neupde: Neural network based ordinary and partial differential equations for modeling time-dependent data, in: *Mathematical and Scientific Machine Learning*, PMLR, 2020, pp. 352–372.
- [29] V. Jayasundara, S. Jayasekara, H. Jayasekara, J. Rajasegaran, S. Seneviratne, R. Rodrigo, Textcaps: Handwritten character recognition with very small datasets, in: 2019 IEEE Winter Conference on Applications of Computer Vision (WACV), IEEE, 2019. doi:10.1109/wacv.2019.00033.
- [30] H. Kabir, M. Abdar, S. M. J. Jalali, A. Khosravi, A. F. Atiya, S. Nahavandi, D. Srinivasan, Spinalnet: Deep neural network with gradual input, arXiv preprint arXiv:2007.03347 (2020).
- [31] A. Nøkland, L. H. Eidnes, Training neural networks with local error signals, in: International Conference on Machine Learning, PMLR, 2019, pp. 4839–4850.
- [32] S. Sabour, N. Frosst, G. E. Hinton, Dynamic routing between capsules, in: *Advances in neural information processing systems*, 2017, pp. 3856–3866.
- [33] H. Xiao, K. Rasul, R. Vollgraf, Fashion-mnist: a novel image dataset for benchmarking machine learning algorithms (2017). arXiv:cs.LG/1708.07747.
- [34] Z. Zhong, L. Zheng, G. Kang, S. Li, Y. Yang, Random erasing data augmentation, in: *Proceedings of the AAAI Conference on Artificial Intelligence*, Vol. 34, 2020, pp. 13001–13008.
- [35] H. Xiao, K. Rasul, R. Vollgraf, Fashion-mnist: a novel image dataset for benchmarking machine learning algorithms, *CoRR* (2017).
- [36] P. Foret, A. Kleiner, H. Mobahi, B. Neyshabur, Sharpness-aware minimization for efficiently improving generalization, in: *International Conference on Learning Representations*, 2021. URL <https://openreview.net/forum?id=6Tm1mposrM>
- [37] K. He, X. Zhang, S. Ren, J. Sun, Deep residual learning for image recognition, in: *Proceedings of the IEEE conference on computer vision and pattern recognition*, 2016, pp. 770–778.
- [38] J. Rajasegaran, V. Jayasundara, S. Jayasekara, H. Jayasekara, S. Seneviratne, R. Rodrigo, Deepcaps: Going deeper with capsule networks, in: *Proceedings of the IEEE Conference on Computer Vision and Pattern Recognition*, 2019, pp. 10725–10733.
- [39] N. H. Phong, B. Ribeiro, Rethinking recurrent neural networks and other improvements for image classification, arXiv preprint arXiv:2007.15161 (2020).
- [40] A. Krizhevsky, G. Hinton, et al., Learning multiple layers of features from tiny images (2009).
- [41] R. D. Hjelm, A. Fedorov, S. Lavoie-Marchildon, K. Grewal, P. Bachman, A. Trischler, Y. Bengio, Learning deep representations by mutual information estimation and maximization, arXiv preprint arXiv:1808.06670 (2018).
- [42] L. Hertel, E. Barth, T. Käster, T. Martinetz, Deep convolutional neural networks as generic feature extractors, in: 2015 International Joint Conference on Neural Networks (IJCNN), 2015, pp. 1–4. doi:10.1109/IJCNN.2015.7280683.
- [43] A. Makhzani, J. Shlens, N. Jaitly, I. Goodfellow, B. Frey, Adversarial autoencoders, arXiv preprint arXiv:1511.05644 (2015).
- [44] V. Dumoulin, I. Belghazi, B. Poole, O. Mastropietro, A. Lamb, M. Arjovsky, A. Courville, Adversarially learned inference, arXiv preprint arXiv:1606.00704 (2016).
- [45] A. Radford, L. Metz, S. Chintala, Unsupervised representation learning with deep convolutional generative adversarial networks, arXiv preprint arXiv:1511.06434 (2015).
- [46] I. Sato, H. Nishimura, K. Yokoi, Apac: Augmented pattern classification with neural networks, arXiv preprint arXiv:1505.03229 (2015).
- [47] Z. Liao, G. Carneiro, On the importance of normalisation layers in deep learning with piecewise linear activation units, in: 2016 IEEE Winter Conference on Applications of Computer Vision (WACV), IEEE, 2016, pp. 1–8.
- [48] G.-J. Qi, Loss-sensitive generative adversarial networks on lipschitz densities, *International Journal of Computer Vision* 128 (5) (2020) 1118–1140.
- [49] C.-Y. Lee, S. Xie, P. Gallagher, Z. Zhang, Z. Tu, Deeply-supervised nets, in: *Artificial intelligence and statistics*, PMLR, 2015, pp. 562–570.
- [50] M. Courbariaux, Y. Bengio, J.-P. David, Binaryconnect: Training deep neural networks with binary weights during propagations, in: NIPS, 2015.
- [51] D. Berthelot, N. Carlini, I. Goodfellow, N. Papernot, A. Oliver, C. A. Raffel, Mixmatch: A holistic approach to semi-supervised learning, in: *Advances in Neural Information Processing Systems*, Vol. 32, Curran Associates, Inc., 2019.
- [52] D. Misra, Mish: A self regularized non-monotonic neural activation function (2020).
- [53] Z. Huang, S. Liang, M. Liang, H. Yang, Dianet: Dense-and-implicit attention network, in: *Proceedings of the AAAI Conference on Artificial Intelligence*, Vol. 34, 2020, pp. 4206–4214.
- [54] K. He, X. Zhang, S. Ren, J. Sun, Identity mappings in deep residual networks, in: *European conference on computer vision*, Springer, 2016, pp. 630–645.
- [55] I. Higgins, L. Matthey, A. Pal, C. Burgess, X. Glorot, M. Botvinick, S. Mohamed, A. Lerchner, beta-vae: Learning basic visual concepts with a constrained variational framework, in: *International Conference on Learning Representations (ICLR)*, 2017.
- [56] A. A. Alemi, I. Fischer, J. V. Dillon, K. Murphy, Deep variational information bottleneck, arXiv preprint arXiv:1612.00410 (2016).

- [57] E. Oyallon, E. Belilovsky, S. Zagoruyko, Scaling the scattering transform: Deep hybrid networks, in: Proceedings of the IEEE international conference on computer vision, 2017, pp. 5618–5627.
- [58] J. Hoffman, E. Tzeng, T. Park, J.-Y. Zhu, P. Isola, K. Saenko, A. Efros, T. Darrell, Cycada: Cycle-consistent adversarial domain adaptation, in: International conference on machine learning, PMLR, 2018, pp. 1989–1998.
- [59] D. Hendrycks, K. Gimpel, A baseline for detecting misclassified and out-of-distribution examples in neural networks, in: International Conference on Learning Representations (ICLR), 2017.
- [60] J. Carranza-Rojas, S. Calderon-Ramirez, A. Mora-Fallas, M. Granados-Menani, J. Torrents-Barrena, Unsharp masking layer: injecting prior knowledge in convolutional networks for image classification, in: International Conference on Artificial Neural Networks, Springer, 2019, pp. 3–16.
- [61] G. Huang, Y. Sun, Z. Liu, D. Sedra, K. Q. Weinberger, Deep networks with stochastic depth, in: European conference on computer vision, Springer, 2016, pp. 646–661.
- [62] D.-A. Clevert, T. Unterthiner, S. Hochreiter, Fast and accurate deep network learning by exponential linear units (elus), arXiv preprint arXiv:1511.07289 (2015).
- [63] E. Real, S. Moore, A. Selle, S. Saxena, Y. L. Suematsu, J. Tan, Q. V. Le, A. Kurakin, Large-scale evolution of image classifiers, in: International Conference on Machine Learning, PMLR, 2017, pp. 2902–2911.
- [64] A. Coates, A. Ng, H. Lee, An analysis of single-layer networks in unsupervised feature learning, in: Proceedings of the fourteenth international conference on artificial intelligence and statistics, 2011, pp. 215–223.
- [65] D. P. Kingma, M. Welling, Auto-encoding variational bayes, arXiv preprint arXiv:1312.6114 (2013).
- [66] C. Luo, J. Zhan, L. Wang, W. Gao, Extended batch normalization, arXiv preprint arXiv:2003.05569 (2020).
- [67] L. Ruthotto, E. Haber, Deep neural networks motivated by partial differential equations, *Journal of Mathematical Imaging and Vision* (2019) 1–13.
- [68] K. Sohn, D. Berthelot, N. Carlini, Z. Zhang, H. Zhang, C. A. Raffel, E. D. Cubuk, A. Kurakin, C.-L. Li, Fixmatch: Simplifying semi-supervised learning with consistency and confidence, in: H. Larochelle, M. Ranzato, R. Hadsell, M. F. Balcan, H. Lin (Eds.), *Advances in Neural Information Processing Systems*, Vol. 33, Curran Associates, Inc., 2020, pp. 596–608.
- [69] I. Sosnovik, M. Szmaja, A. Smeulders, Scale-equivariant steerable networks, in: International Conference on Learning Representations, 2019.
- [70] Z. Lu, K. Deb, E. Goodman, W. Banzhaf, V. N. Boddeti, Nsganetv2: Evolutionary multi-objective surrogate-assisted neural architecture search, in: European Conference on Computer Vision, Springer, 2020, pp. 35–51.
- [71] K. Saito, Y. Ushiku, T. Harada, Asymmetric tri-training for unsupervised domain adaptation, arXiv preprint arXiv:1702.08400 (2017).
- [72] B. B. Moser, F. Raue, J. Hees, A. Dengel, Dartsnet: Exploring new rnn cells in renet architectures, in: I. Farkaš, P. Masulli, S. Wermter (Eds.), *Artificial Neural Networks and Machine Learning – ICANN 2020*, Springer International Publishing, Cham, 2020, pp. 850–861.
- [73] D. Hendrycks, M. Mazeika, T. Dietterich, Deep anomaly detection with outlier exposure, in: International Conference on Learning Representations, 2019.
- [74] S. Zagoruyko, N. Komodakis, Wide residual networks, arXiv preprint arXiv:1605.07146 (2016).
- [75] M. Farhadi, M. Ghasemi, Y. Yang, A novel design of adaptive and hierarchical convolutional neural networks using partial reconfiguration on fpga, in: 2019 IEEE High Performance Extreme Computing Conference (HPEC), IEEE, 2019, pp. 1–7.
- [76] A. Ju, D. Wagner, E-abs: Extending the analysis-by-synthesis robust classification model to more complex image domains, in: Proceedings of the 13th ACM Workshop on Artificial Intelligence and Security, 2020, pp. 25–36.
- [77] Y. Ganin, E. Ustinova, H. Ajakan, P. Germain, H. Larochelle, F. Laviolette, M. Marchand, V. Lempitsky, Domain-adversarial training of neural networks, *The Journal of Machine Learning Research* 17 (1) (2016) 2096–2030.
- [78] P. Haeusser, T. Frerix, A. Mordvintsev, D. Cremers, Associative domain adaptation, in: Proceedings of the IEEE International Conference on Computer Vision, 2017, pp. 2765–2773.
- [79] G. French, M. Mackiewicz, M. Fisher, Self-ensembling for visual domain adaptation, arXiv preprint arXiv:1706.05208 (2017).
- [80] S. Roy, A. Siarohin, E. Sangineto, S. R. Bulo, N. Sebe, E. Ricci, Unsupervised domain adaptation using feature-whitening and consensus loss, in: Proceedings of the IEEE Conference on Computer Vision and Pattern Recognition, 2019, pp. 9471–9480.